Lake, R. E.; Arista, N.R.

Kinetic-energy transfer in highly-charged-ion collisions with carbon

Published in:
Physical Review A

DOI:
10.1103/PhysRevA.92.052710

Published: 01/01/2015

Document Version
Publisher's PDF, also known as Version of record

Kinetic-energy transfer in highly-charged-ion collisions with carbon

R. E. Lake[1,*] and N. R. Arista[2]

[1]*COMP Centre of Excellence, Department of Applied Physics, Aalto University, FI-00076 Aalto, Finland*

[2]*División Colisiones Atómicas, Instituto Balseiro and Centro Atómico Bariloche, Comisión Nacional de Energía Atómica, 8400 San Carlos de Bariloche, Argentina*

(Received 16 June 2015; revised manuscript received 27 August 2015; published 23 November 2015)

We present an accurate theoretical model for the charge dependence of kinetic energy transferred in collisions between slow highly charged ions (HCIs) and the atoms in a carbon solid. The model is in excellent agreement with experimental kinetic-energy-loss data for carbon nanomembrane and thin carbon foil targets. This study fills a notable gap in the literature of charged-particle energy loss in the regime of low incident velocity ($v_p \lesssim 2.188 \times 10^6$ m/s) where charge states greatly exceed the equilibrium values.

DOI: 10.1103/PhysRevA.92.052710 PACS number(s): 34.50.Bw, 34.35.+a, 61.85.+p, 79.20.Rf

Accurate descriptions of interactions between energetic ions and matter have provided tools for modifying and probing solids at the atomic scale. Extensive theoretical and experimental work has given rise to a multitude of applications that are ubiquitous throughout micro- and nano-electronics fabrication, including ion etching, milling, and patterning of materials [1,2]. A remarkable demonstration of the sophistication reached in this field is the use of controlled ion implantation to realize atom-sized quantum circuit elements [3–9]. Theories of ion energy loss provide the crucial input parameters (e.g., stopping ranges, damage thresholds, straggling distributions, atomic displacement densities) needed to deterministically implant single ions in solids and play an important role in the growth of this new area of physics [10]. For ions with low charge states, existing mathematical and semi-empirical models explain the kinetic-energy loss for nearly all possible projectile-target combinations for several orders of magnitude in incident-ion energy [11].

A knowledge gap exists in understanding the role of projectile charge states Q in the stopping of slow highly charged ions (HCIs) in the regime where nuclear collisions are the dominant energy-transfer channel. In particular, the largest deviations from existing stopping-power models occur for "heavy" projectiles (nuclear charge $Z_p \gg 1$) with high charge states ($Q \gg 1$) at low velocities ($v_p < 1$) [12,13]. Strong enhancements in kinetic-energy loss have been predicted [14] and observed [15–17] when Q greatly exceeds the ion equilibrium charge states although the mechanism for the enhancement remains unclear. Several experiments motivate a systematic treatment of charge-dependent kinetic-energy transfer in nuclear recoil cascades formed by HCIs. Transmission energy loss measurements with conducting and insulating foils and membranes reveal enhancements in kinetic-energy loss as Q increases [15–17]. Additionally, charge-dependent compression of stopping ranges has been observed in depth-resolved measurements of ions implanted in insulators, indicating increased stopping power for increased charge states prior to charge equilibration (see Fig. 4 in Ref. [18]). Finally, there is preliminary evidence of increased damage to dielectric thin-film targets for decreased HCI velocities in tunnel junction sensors [19]. Many previous studies have focused on intense electronic excitations due to charge-dependent potential-energy deposition and subsequent defect formation associated with HCI neutralization [13,20–24]. On the other hand, charge-dependent kinetic-energy transfer and synergistic effects [25] between potential and kinetic energy have only recently gained attention. These phenomena are increasingly relevant since bright sources of slow HCIs are available [26–29] and provide a direct means of accessing the regime ($Q \gg 1$, $v_p < 1$) experimentally.

In this article we present an accurate model for charge-dependent nuclear energy transfer for HCIs (Au^{Q+}, Xe^{Q+}, Kr^{Q+}, Ar^{Q+}, and O^{Q+}) interacting with C targets. The model is based on the analytical Dirac–Hartree–Fock–Slater (DHFS) screening function for C target atoms and uses the Brandt–Kitagawa ion model (BK) to treat screening from the projectile ion's electronic structure [30]. We obtain charge-dependent kinetic-energy transfer as a function of impact parameter and integrate over impact parameter to derive Q-dependent stopping from multiple binary collisions. The electronic stopping contribution is included with the nonlinear method for slow ions [31].

We compare the model to two key transmission energy loss datasets with C nanomembrane ($\Delta x \approx 10$ Å) [16] and self-supported C foil targets ($\Delta x \approx 100$ Å) [15] and demonstrate excellent agreement with the experiments. The data considered from Ref. [16] were obtained with HCI beams at normal incidence to a nanomembrane target with detector observation angles around 0° and constant exit charge state $Q_{\rm exit} = 2$. The distribution of detected ions is heavily weighted by small scattering angles from single-collision trajectories [16,32]. In contrast, data from Ref. [15] were obtained for thicker C foil targets where multiple binary collisions along Δx affect the measured energy loss even near the 0° observation angle. All transmission measurements restrict the impact parameters that can be accessed experimentally due to finite detector acceptance. However, for the case of projectile ions heavier than target atoms, even the most violent collisions result in projectile motion along the forward direction [33] so that the close collisions relevant to stopping can be probed in transmission. Importantly, these datasets [15,16] are a test bed for developing an ion-solid interaction model that reproduces charge-dependent kinetic-energy transfer under a well-defined experimental geometry.

*russell.lake@aalto.fi

We begin by calculating charge-dependent kinetic energy transfer $T(Q,b)$ from a projectile ion with charge state Q and incident energy $E_p = M_p v_p^2/2$ (in the laboratory frame) to a target atom at rest with mass M_t and nuclear charge Z_t. The collision is characterized by impact parameter b. Following the theory of nuclear collisions [34–39], projectile charge is introduced directly into the scattering potential. We construct the scattering potential from the analytical DHFS screening function ($\phi_{\rm HF}$) [40,41] for C ($A_1 = 0.1537$, $A_2 = 0.8463$, $\alpha_1 = 8.0404$, $\alpha_2 = 1.4913$) modeled here as

$$V_{\rm HF} = \frac{Z_t Q_{\rm eff}}{r}\phi_{\rm HF},$$
$$\phi_{\rm HF} = A_1 \exp(-\alpha_1 r) + A_2 \exp(-\alpha_2 r), \tag{1}$$

where r is the distance from the target atom to the projectile ion. The main screening effect is provided by the potential of the C atom, with range determined by $\phi_{\rm HF}$. Specifically, the screening distance $a_s = \alpha_2^{-1} \approx 0.67 \approx 0.35$ Å defines a characteristic length to separate close from distant collisions (or small and large impact parameters). The fact that a_s is much smaller than the distance between neighboring C atoms enables the use of the binary-collision approximation.

In Eq. (1), $Q_{\rm eff}$ is the effective charge of the projectile ion given by

$$Q_{\rm eff}(r) = Z_p - \int_0^r n_e^{(Q)}(r')4\pi r'^2 dr', \tag{2}$$

where $n_e^{(Q)}(r)$ is the projectile ion electronic charge density, which is represented by using BK [30]. At long range the projectile ion can be considered a point charge: $Q_{\rm eff} \to Q$. At close range the effect of screening due to electronic structure becomes significant. Equation (1) captures the strong interactions dominated by a screened Coulomb repulsion between ion-atom pairs at close and intermediate distances. Attractive interactions from long-range polarization effects do not play a significant role in energy transfer and are disregarded.

From $V_{\rm HF}$ we obtain the scattering angle in the collision center-of-mass (CM) frame as a function of impact parameter and projectile charge state, i.e., $\theta(Q,b)$. The energy transfer is directly related to $\theta(Q,b)$ as [33]

$$T(Q,b) = T_{\rm max} \sin^2\left[\frac{\theta(Q,b)}{2}\right], \tag{3}$$

where $T_{\rm max} = 4E_p M_p M_t (M_p + M_t)^{-2}$. Therefore, the problem of calculating $T(Q,b)$ reduces to finding the scattering angle after each collision.

For small scattering angles $\theta_{\rm SA}$, Lindhard *et al.* [42] provided the analytical approximation,

$$\theta_{\rm SA}^2(Q,b) = -\frac{3}{(M_{\rm r} v^2)^2} b^{\frac{1}{3}} \frac{d}{db}\left\{V_{\rm HF}^2(Q) b^{\frac{2}{3}}\right\}, \tag{4}$$

where $M_{\rm r} = M_t M_p (M_t + M_p)^{-1}$ is the reduced mass. Considering Eq. (3) in the small-angle limit and substituting Eq. (4), the energy transfer in a single collision is well approximated by $T \cong T_{\rm max}\theta_{\rm SA}^2/4$.

The validity of Eq. (4) is restricted to small angles, corresponding to large impact parameters. To obtain an accurate description of energy transfer for small impact parameters ($b < a_s$) we consider the exact calculation of angular dispersion (in the binary collision approximation) by integrating the classical trajectories. In this approach $\theta(Q,b)$ is obtained by integrating the trajectory of the relative motion during the collision [43],

$$\theta_{\rm ex}(Q,b) = \pi - 4b\int_0^1 \frac{du}{\sqrt{f(u,b,V_{\rm HF},E_{\rm CM})}}. \tag{5}$$

Here, f is a function that depends on impact parameter, scattering potential, and kinetic energy in the CM frame [43]. Thus, energy transfer may be evaluated by using Eq. (3) with $\theta_{\rm ex}$ from Eq. (5) and is valid at arbitrary impact parameters in a binary collision.

For nanomembrane targets Eqs. (4) and (5) correspond directly to the measured mean kinetic-energy loss (ΔE) from single collisions [16]. For the foil targets [15], the nuclear stopping contribution to ΔE is calculated by integrating $T(Q,b)$ over the range of impact parameters in multiple collisions within the target of atomic density $N = 0.977 \times 10^{23}$ cm^{-3},

$$S_n(Q) = N\int_{b_{\rm min}}^{b_{\rm max}} T(Q,b) 2\pi b db. \tag{6}$$

In Eq. (6) the lower limit is $b_{\rm min} = 0$, while the upper limit is half the mean distance between neighboring C atoms; $b_{\rm max} = 0.7$ Å. The mean energy loss due to nuclear collisions within the target of thickness Δx is $S_n(Q)\Delta x$. In addition, we introduce electronic stopping [$S_e(Q)$] via nonlinear calculations for slow ions, as detailed in Ref. [31].

Figure 1(a) shows the comparison between the calculated and measured energy loss of $Xe^{Q+}(10 \leqslant Q \leqslant 30)$ projectiles transmitted through C nanomembranes with $E_p = 40$ keV at small observation angles [16]. The ΔE data are dominated by

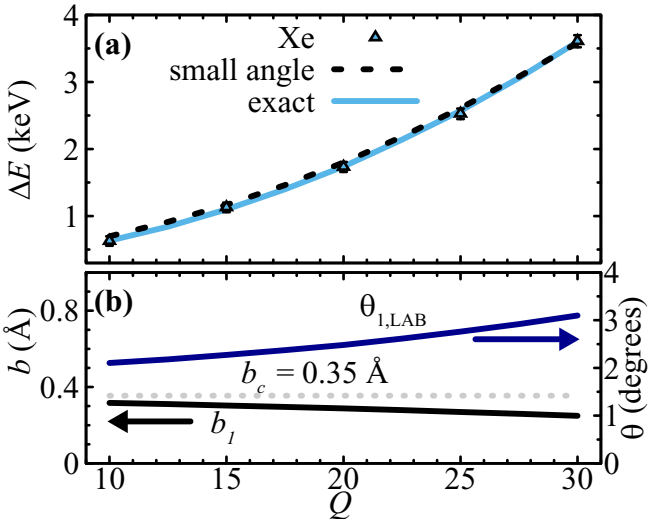

FIG. 1. (Color online) (a) Mean energy loss of Xe^{Q+} transmitted through C nanomembranes. Triangles are data from Fig. 3(b) in Ref. [16] ($E_p = 40$ keV). Dashed and solid lines are calculated from $T(Q,b)$ by using the small-angle approximation [Eqs. (3) and (4)] and exact calculation [Eqs. (3) and (5)], respectively. (b) Impact parameters extracted from fits to data: b_c from the small-angle approximation and b_1 from the exact calculation (left axis). $\theta_{1,\rm LAB}$ is the scattering angle in the laboratory frame for impact parameter b_1 (right axis).

single Xe^{Q+}–C collisions [16,32]. Therefore, we model ΔE with Eq. (3). Specifically, Eq. (3) is calculated with both the small-angle approximation in Eq. (4) and the exact scattering formulation in Eq. (5). With the small-angle approximation of Eqs. (3) and (4), the model fits the ΔE data points with a single impact parameter $b_c = 0.35$ Å. Figure 1(a) shows excellent agreement between $T(Q,b_c)$ (dashed line) and the ΔE data points. With the exact scattering formulation of Eqs. (3) and (5), the best fit to ΔE is obtained with impact parameters in the range 0.25 Å $< b_1 < 0.32$ Å. The results of this calculation, $T(Q,b_1)$, are plotted as the solid line in Fig. 1(a) and also provide excellent agreement with the ΔE data. Figure 1(b) displays the impact parameters extracted from a fit to each $T(Q,b)$ calculation (left axis). As an additional check, we calculate dispersion angles of the Xe ions in the laboratory frame ($\theta_{1,\mathrm{LAB}}$) and plot the values in Fig. 1(b) (right axis). The values ($2^\circ < \theta_{1,\mathrm{LAB}} < 3^\circ$) are within the bounds obtained in Ref. [16] that the Xe-C collisions "...yield a maximum deflection angle of 5.2° for one elastic scattering event."

For experiments with Xe^{Q+} projectiles transmitted through C nanomembranes [Fig. 1(a)], the data can be accurately modeled with both calculations: (i) the small-angle approximation with a single impact parameter $b_c = 0.35$ Å, or (ii) the exact scattering formulation with impact parameters in the range $b_1 = 0.25$ Å to $b_1 = 0.32$ Å. Considering the radial wave functions of neutral C reported in Ref. [44], these impact parameters correspond to ion trajectories that penetrate the maximum electron density of the L shell of C atoms. The data in Fig. 1(a) represent the energy loss of "ions with the highest charge loss observable" in the setup of Ref. [16]. Therefore our model reveals that the ions suffering the highest charge loss are those that undergo close collisions with the L shell electrons of C. As discussed below, the energy transferred in collisions with these impact parameters have a strong dependence on Q.

Figure 2 shows both the calculated and measured ΔE of Au^{Q+}, Xe^{Q+}, Kr^{Q+}, Ar^{Q+}, and O^{Q+} transmitted through C foils with effective thickness $\Delta x = 104$ Å [15]. Energy loss from nuclear collisions $S_n(Q)\Delta x$ is calculated by using the exact scattering formulation of Eqs. (3), (5), and (6) [dashed lines in Figs. 2(a) and 2(b)] and the contribution from electronic stopping $S_e(Q)$ [31] is included. Thus, the mean kinetic-energy loss is modeled as $\Delta E = [S_n(Q) + S_e(Q)]\Delta x$ [solid lines in Figs. 2(a) and 2(b)]. As shown in Fig. 2, the theoretically obtained values of Q-dependent ΔE are in excellent agreement for all atomic species considered.

An essential point is that Figs. 1 and 2 show very different behavior with respect to Q-dependent energy loss. In particular—for Xe^{Q+} in Fig. 2(a)—a relatively flat dependence of ΔE is observed in the low-Q regime: there is a mere 10% increase in the calculated nuclear energy loss (dashed line) between $Q = 10$ and $Q = 30$. In contrast—for Xe^{Q+} transmitted through C nanomembranes [Fig. 1(a)]—ΔE increases by 470% over the same variation in Q. The quadratic charge-dependent enhancement in ΔE for C nanomembranes is observed in both the data and calculation in Fig. 1(a). To understand the difference in charge dependence of ΔE between datasets in Fig. 1(a) and Fig. 2, we analyze the behavior of $T(Q,b)$.

We consider the question of which collisions (close versus distant) provide the dominant contribution to HCI energy loss in C. Figure 3(a) displays $T(Q,b)$ as a function of impact parameter for Xe^{Q+} with charge states $Q = 10$, $Q = 20$, $Q = 30$, and $Q = 54$ ($E_p = 312.4$ keV). As impact parameter increases, $T(Q,b)$ decreases by more than an order of magnitude in the relevant range 0 Å $< b < 0.5$ Å, for all charge states. In the limit $b \to 0$, all charge states converge to a single curve: $T(Q,b)$ saturates at $T_{\max}$ and has no dependence on Q. It is also instructive to look at the behavior of $Q_{\mathrm{eff}}(b)$ in Fig. 3(b). In the close collision regime of low-b values, screening due to the ion's electronic structure does not affect the Coulombic repulsion between the HCI and C atom. Equivalently, $Q_{\mathrm{eff}}(b)$ approaches the nuclear charge Z_p as the interaction distance becomes small in Eq. (2) and the HCI behaves as a point charge $Q_{\mathrm{eff}}(r) \simeq Z_p$. As shown in Fig. 3(b)—in the opposite impact-parameter regime of distant collisions—the effective charge approaches the HCI charge state as $Q_{\mathrm{eff}}(r) \simeq Q$ and the projectile's ionization state plays a significant role in the interaction.

The strong Q-dependent increase in energy loss observed in the data of Fig. 1(a) can be understood by considering that the extracted impact parameters from the exact $T(Q,b_1)$ calculation are in the range 0.25 Å $< b_1 < 0.32$ Å in Figs. 3(a) and 3(b). In these collisions, the energy transfer increases quadratically with increasing Q. The same conclusions hold for $b_c = 0.35$ Å extracted from the fit by using the small-angle-approximation calculation. Here we note that the small-angle approximation also reproduces the quadratic scaling of $T(Q,b)$ and that this scaling can be derived analytically from Eqs. (1) and (4) considering the effective charge at the impact parameter $b_c = 0.35$ Å ($Q_{\mathrm{eff}} \to Q$).

Experiments of Ref. [15] reveal information on the stopping that results from multiple collisions with C atoms in the foil with a variety of impact parameters. Figure 3 gives insight

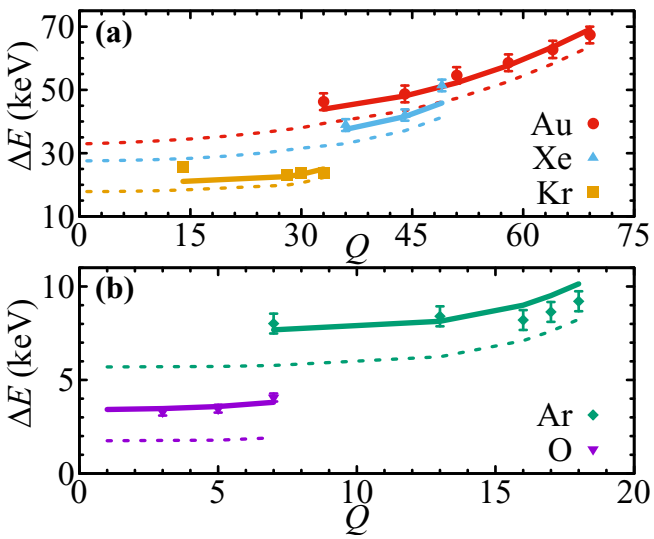

FIG. 2. (Color online) Mean energy loss of (a) Au^{Q+}, Xe^{Q+}, Kr^{Q+} and (b) Ar^{Q+}, O^{Q+} with $v_p \approx 0.3$ [Xe^{Q+}: $E_p = (312.4 \pm 2)$ keV] transmitted through C foils ($\Delta x = 104$ Å) [15]. Markers are data, solid lines are calculations of $(S_n + S_e)\Delta x$, and dashed lines are calculations of $S_n \Delta x$.

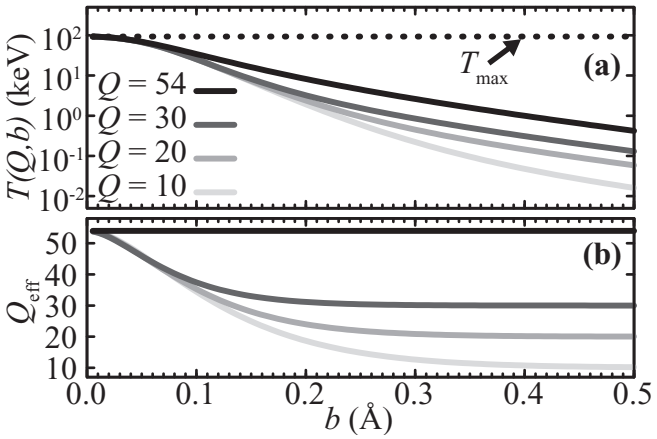

FIG. 3. (a) Calculated $T(Q,b)$ for Xe^{Q+} at $E_p = 312.4$ keV. The dashed line indicates T_{max}. (b) $Q_{eff}(b)$ from Eq. (2) plotted for the same Q as in panel (a).

into the relatively weak Q dependence of ΔE. As seen from the rapid decay of $T(Q,b)$ with increasing impact parameter [Fig. 3(a)], the dominant contribution to the stopping-power integral in Eq. (6) comes from the energy transferred in close collisions ($b \to 0$). In this the close collision regime, the value of effective charge nearly saturates as $Q_{eff}(r) \simeq Z_p$ so that both $T(Q,b)$ and the resulting mean energy losses depend more sensitively on Z_p than on Q. Quantitatively, for Xe^{Q+} over the range $Q = 10$ to $Q = 54$ at $v_p \approx 0.3$, the fraction of the total kinetic-energy loss coming from close collisions ($b < 0.26$ Å) varies from 98% to 80%. Close collisions dominate the total energy loss and the energy transfer in these collisions is only weakly dependent on Q [Fig. 3(a)].

Equation 6 includes no assumption about charge equilibration time: Q is modeled as constant in each collision. Therefore, the agreement between the calculation and data in Fig. 2 can be interpreted in two ways: (1) subsurface electron capture does not directly interfere with the close collisions that dominate the energy transfer; (2) projectile electronic equilibration time in C is long compared to the transit time across $\Delta x \approx 100$ Å. Regarding the latter possibility, x-ray spectroscopy of HCIs within metallic foils (Pb^{54+}; $v_p = 0.3$) shows that even M shell vacancies can survive at penetration depths of a few tens of nanometers [45]. In this way it is possible that collisions between nonequilibrium projectiles and atoms are characterized by initial charge Q within the first several nanometers of a solid even as smaller exit charges are measured outside the solid.

In summary, our theoretical approach quantitatively describes experiments on HCIs interacting with C under different conditions: (i) energy transfer in single collisions with nanomembranes, and (ii) stopping in thin foils. The model explains the Q dependence of ΔE in both (i) and (ii) and provides microscopic information on the interaction with target atoms through the extracted impact-parameter values. The largest Q-dependent enhancements in energy transfer are observed for intermediate and distant collisions [$b > 0.2$ Å in Fig. 3(a)]. For C foil targets, the influence of distant collisions on the total energy loss is quenched by the short screening range of V_{HF}, producing a weak Q dependence of the stopping. These results imply that even larger Q-dependent enhancements in energy transfer from nuclear collisions will be observed for high impact parameters in cases where screening effects are suppressed. Such conditions may be obtained by choosing nonconducting target materials.

R.E.L. acknowledges support from Academy of Finland No. 265675. N.R.A. acknowledges support from ANPCYT, Argentina (PICT 124/2012).

[1] E. Chason, S. T. Picraux, J. M. Poate, J. O. Borland, M. I. Current, T. D. de la Rubia, D. J. Eaglesham, O. W. Holland, M. E. Law, C. W. Magee, J. W. Mayer, J. Melngailis, and A. F. Tasch, J. Appl. Phys. **81**, 6513 (1997).
[2] M. Ieong, B. Doris, J. Kedzierski, K. Rim, and M. Yang, Science **306**, 2057 (2004).
[3] T. Schenkel, A. Persaud, S. J. Park, J. Nilsson, J. Bokor, J. A. Liddle, R. Keller, D. H. Schneider, D. W. Cheng, and D. E. Humphries, J. Appl. Phys. **94**, 7017 (2003).
[4] G. P. Lansbergen, R. Rahman, C. J. Wellard, I. Woo, J. Caro, N. Collaert, S. Biesemans, G. Klimeck, L. C. L. Hollenberg, and S. Rogge, Nat. Phys. **4**, 656 (2008).
[5] C. Yin, M. Rancic, G. G. de Boo, N. Stavrias, J. C. McCallum, M. J. Sellars, and S. Rogge, Nature (London) **497**, 91 (2013).
[6] F. A. Zwanenburg, A. S. Dzurak, A. Morello, M. Y. Simmons, L. C. L. Hollenberg, G. Klimeck, S. Rogge, S. N. Coppersmith, and M. A. Eriksson, Rev. Mod. Phys. **85**, 961 (2013).
[7] J. van Donkelaar, C. Yang, A. D. C. Alves, J. C. McCallum, C. Hougaard, B. C. Johnson, F. E. Hudson, A. S. Dzurak, A. Morello, D. Spemann, and D. N. Jamieson, J. Phys.: Condens. Matter **27**, 154204 (2015).
[8] S. Pezzagna, D. Wildanger, P. Mazarov, A. D. Wieck, Y. Sarov, I. Rangelow, B. Naydenov, F. Jelezko, S. W. Hell, and J. Meijer, Small **6**, 2117 (2010).
[9] I. Aharonovich, A. D. Greentree, and S. Prawer, Nat. Photonics **5**, 397 (2011).
[10] *Single-Atom Nanoelectronics*, edited by E. Prati and T. Shinada (Pan Stanford Publishing, Singapore, 2013).
[11] J. Ziegler, J. Biersack, and U. Littmark, *The Stopping and Ranges of Ions in Matter* (Pergamon, New York, 1985).
[12] Atomic units (a.u.) are used except where noted—velocity: 1 a.u. $\approx 2.188 \times 10^6$ m/s; charge: 1 a.u. $\approx 1.602 \times 10^{-19}$ C; length: 1 a.u. $\approx 0.5292 \times 10^{-10}$ m, and 1 Å $\equiv 10^{-10}$ m; energy: 1 a.u. $\approx 4.360 \times 10^{-18}$ J, and 1 eV $\approx 1.602 \times 10^{-19}$ J.
[13] T. Schenkel, A. V. Hamza, A. V. Barnes, and D. H. Schneider, Prog. Surf. Sci. **61**, 23 (1999).
[14] J. P. Biersack, Nucl. Instrum. Methods Phys. Res., Sect. B **80-81**, 12 (1993).

[15] T. Schenkel, M. A. Briere, A. V. Barnes, A. V. Hamza, K. Bethge, H. Schmidt-Böcking, and D. H. Schneider, Phys. Rev. Lett. **79**, 2030 (1997).
[16] R. A. Wilhelm, E. Gruber, R. Ritter, R. Heller, S. Facsko, and F. Aumayr, Phys. Rev. Lett. **112**, 153201 (2014).
[17] M. A. Briere, T. Schenkel, D. H. Schneider, P. Bauer, and A. Arnau, Phys. Scr. **1997**, 324 (1997).
[18] T. Schenkel, C. Lo, C. Weis, A. Schuh, A. Persaud, and J. Bokor, Nucl. Instrum. Methods Phys. Res., Sect. B **267**, 2563 (2009).
[19] J. M. Pomeroy and R. E. Lake, Nucl. Instrum. Methods Phys. Res., Sect. B **317**, 66 (2013).
[20] M. Tona, H. Watanabe, S. Takahashi, N. Nakamura, N. Yoshiyasu, M. Sakurai, T. Terui, S. Mashiko, C. Yamada, and S. Ohtani, Surf. Sci. **601**, 723 (2007).
[21] A. S. El-Said, R. Heller, W. Meissl, R. Ritter, S. Facsko, C. Lemell, B. Solleder, I. C. Gebeshuber, G. Betz, M. Toulemonde, W. Möller, J. Burgdörfer, and F. Aumayr, Phys. Rev. Lett. **100**, 237601 (2008).
[22] R. Heller, S. Facsko, R. A. Wilhelm, and W. Moller, Phys. Rev. Lett. **101**, 096102 (2008).
[23] M. Tona, Y. Fujita, C. Yamada, and S. Ohtani, Phys. Rev. B **77**, 155427 (2008).
[24] R. E. Lake, J. M. Pomeroy, H. Grube, and C. E. Sosolik, Phys. Rev. Lett. **107**, 063202 (2011).
[25] Y. Y. Wang, C. Grygiel, C. Dufour, J. R. Sun, Z. G. Wang, Y. T. Zhao, G. Q. Xiao, R. Cheng, X. M. Zhou, J. R. Ren, S. D. Liu, Y. Lei, Y. B. Sun, R. Ritter, E. Gruber, A. Cassimi, I. Monnet, S. Bouffard, F. Aumayr, and M. Toulemonde, Sci. Rep. **4**, 5742 (2014).
[26] X. Ma, H. P. Liu, L. T. Sun, M. T. Song, X. L. Zhu, S. Sha, W. T. Feng, D. C. Zhang, S. F. Zhang, B. Li, J. Y. Li, D. B. Qian, S. Y. Xu, D. Q. Gao, P. Z. Wang, L. Z. Ma, K. D. Man, G. Q. Xiao, H. W. Zhao, and W. L. Zhan, J. Phys.: Conf. Ser. **163**, 012104 (2009).
[27] G. Zschornack, M. Kreller, V. P. Ovsyannikov, F. Grossman, U. Kentsch, M. Schmidt, F. Ullmann, and R. Heller, Rev. Sci. Instrum. **79**, 02A703 (2008).
[28] R. Ginzel, S. Higgins, P. Mrowcynski, P. Northway, M. Simon, H. Tawara, J. C. López-Urrutia, J. Ullrich, G. Kowarik, R. Ritter, W. Meissl, C. Vasko, C. Gösselsberger, A. El-Said, and F. Aumayr, Nucl. Instrum. Methods Phys. Res., Sect. B **268**, 2972 (2010).
[29] R. Shyam, D. D. Kulkarni, D. A. Field, E. S. Srinadhu, D. B. Cutshall, W. R. Harrell, J. E. Harriss, and C. E. Sosolik, AIP Conf. Proc. **1640**, 129 (2015).
[30] W. Brandt and M. Kitagawa, Phys. Rev. B **25**, 5631 (1982); **26**, 3968 (1982).
[31] N. R. Arista, Nucl. Instrum. Methods Phys. Res., Sect. B **195**, 91 (2002); **207**, 232 (2003).
[32] M. M. Jakas, G. H. Lantschner, J. C. Eckardt, and V. H. Ponce, Phys. Rev. A **29**, 1838 (1984).
[33] L. D. Landau and E. M. Lifshitz, *Mechanics*, 2nd ed. (Pergamon Press, New York, 1969).
[34] N. Bohr, Mat. Fys. Medd. Dan. Vid. Selsk. **18**, 1 (1948).
[35] J. Lindhard, V. Nielsen, M. Scharff, and P. V. Thomsen, Mat. Fys. Dan. Medd. Dan. Vid. Selsk. **33**(10), 1 (1963).
[36] J. Lindhard, M. Scharff, and H. E. Schiøtt, Mat. Fys. Dan. Medd. Dan. Vid. Selsk. **33**(14), 1 (1963).
[37] K. A. Kumakhov and K. Komarov, *Energy Loss and Ion Ranges in Solids* (Gordon and Breach, New York, 1981).
[38] E. Bonderup, *Penetration of Charged Particles through Matter*, Lecture Notes (University of Aarhus, Aarhus, 1981).
[39] P. Sigmund, *Stopping of Heavy Ions: A Theoretical Approach*, Springer Tracts in Modern Physics (Springer, Berlin, 2004).
[40] F. Salvat, J. D. Martínez, R. Mayol, and J. Parellada, Phys. Rev. A **36**, 467 (1987).
[41] I. M. Torrens, *Interatomic Potentials* (Academic Press, Inc., New York, 1972).
[42] J. Lindhard, V. Nielsen, and M. Scharff, Mat. Fys. Medd. Dan. Vid. Selsk. **36**, 1 (1968).
[43] M. T. Robinson, U.S. Atomic Energy Commission Report ORNL-4556 (1970).
[44] R. Thiele, S.-K. Son, B. Ziaja, and R. Santra, Phys. Rev. A **86**, 033411 (2012).
[45] Z. D. Pešić, G. Vikor, S. Atanassova, J. Anton, S. Leontein, M. Björkhage, A. Paál, H. Hanafy, and R. Schuch, Phys. Rev. A **75**, 012903 (2007).